small NANO MICRO

Cellular imaging

DOI: 10.1002/smll.200700054

Dendrimer-Entrapped Gold Nanoparticles as a Platform for Cancer-Cell Targeting and Imaging

Xiangyang Shi, Suhe Wang,* Sasha Meshinchi, Mary E. Van Antwerp, Xiangdong Bi, Inhan Lee, and James R. Baker, Jr.**

We present a general approach for the targeting and imaging of cancer cells using dendrimer-entrapped gold nanoparticles (Au DENPs). Au DENPs were found to be able to covalently link with targeting and imaging ligands for subsequent cancer-cell targeting and imaging. The Au DENPs linked with defined numbers of folic acid (FA) and fluorescein isothiocyanate (FI) molecules are water soluble, stable, and biocompatible. In vitro studies show that the FA- and FI-modified Au DENPs can specifically bind to KB cells (a human epithelial carcinoma cell line) that overexpress high-affinity folate receptors and they are internalized dominantly into lysosomes of target cells within 2 h. These findings demonstrate that Au DENPs may serve as a general platform for cancer imaging and therapeutics.

Keywords:
- cancer
- dendrimers
- gold
- imaging
- nanoparticles

1. Introduction

Dendrimer-entrapped metal nanoparticles are of scientific and technological interest because of their unique structure and functionality.[1–5] These nanoparticles have been primarily used in catalysis,[6] optics,[7] and other applications unrelated to biomedical sciences. The absence of biological applications is largely due to the toxicity of these particles and technical difficulties with their surface manipulation. Dendrimer-entrapped metal nanoparticles (metal DENPs) are usually prepared by reducing metal ions that have been complexed with dendrimer templates.[2,4,6–8] Because of the diameter of the dendrimer template, these particles are always smaller than 3 nm.[6] While there are a few reports on biological sensing using dendrimer-stabilized metal nanoparticles (also called "interdendrimer nanoparticles"),[9,10] there is no reported literature showing that these nanoparticles can achieve specificity and selectivity in biological systems.

In a previous report, we demonstrated that dendrimer-entrapped gold nanoparticles (Au DENPs) prepared using amine-terminated fifth-generation poly(amidoamine) (PAMAM) dendrimers ($G5{\cdot}NH_2$) as templates can be surface-modified with acetyl and hydroxyl groups, thereby significantly reducing the toxicity of Au DENPs.[11] The ability to chemically functionalize preformed Au DENPs without significantly changing their sizes and size distributions led us to develop Au DENPs as a multifunctional platform for cancer-cell targeting, imaging, and treatment as we have carried out with dendrimers.[12–15] It should be possible to visualize Au DENP-based therapeutics in targeted cells and tis-

[*] Dr. X. Shi,[+] Dr. S. Wang,[+] M. E. Van Antwerp, Dr. X. Bi, Prof. J. R. Baker, Jr.
Michigan Nanotechnology Institute for Medicine and Biological Sciences, University of Michigan
Ann Arbor, MI 48109 (USA)
Fax: (+1) 734-615-2506
E-mail: xshi@umich.edu
shidasui@umich.edu
jbakerjr@umich.edu
S. Meshinchi
Department of Cell and Developmental Biology
Medical School, University of Michigan
Ann Arbor, MI 48109 (USA)
Dr. I. Lee
Michigan Center for Biological Information and Department of Psychiatry, University of Michigan
3600 Green Court, Suite 700, Ann Arbor, MI 48105 (USA)
[+] These authors equally contributed to this work.

Supporting information for this article is available on the WWW under http://www.small-journal.com or from the author.

sues because of the high electron-density contrast of the Au atoms. Multifunctional Au DENPs may also be used for targeted hyperthermia treatment of cancers through inductive heating of cells that have internalized these particles.

Here we demonstrate that Au DENPs can be covalently linked with targeting ligands and imaging molecules for cancer-cell targeting and imaging. Au DENPs linked with defined numbers of folic acid (FA) and fluorescein isothiocyanate (FI) molecules are water soluble, stable, and biocompatible. We show that the FA- and FI-modified Au DENPs can specifically bind to KB cells (a human epithelial carcinoma cell line) that overexpress high-affinity folate receptors and be internalized predominantly into lysosomes of target cells within 2 h. These findings document a facile approach to use Au DENPs as a platform for the targeting and imaging of cancer cells.

2. Results

2.1. Surface Modification, Characterization, Stability, and Toxicity of Au DENPs

Au DENPs were prepared using G5·NH_2 dendrimers as templates according to previously described procedures.[8,11,16] The formed Au DENPs are relatively monodisperse with a mean diameter of 2.1 nm.[11] It is worthwhile to note that the size of the synthesized pristine Au DENPs is larger than those particles prepared by Crooks and co-workers.[16] This is presumably due to the difference in the preparation conditions, such as the metal atom/dendrimer molar ratio, type of dendrimer templates, as well as the reaction solvents used. The approach to functionalize Au DENPs with defined numbers of targeting molecules (e.g., FA) and dyes (e.g., FI) is slightly modified from the methods that are used to functionalize dendrimers (without entrapped metal nanoparticles) for targeting and imaging of cancer cells (Figure 1).[13,17,18] One of the key steps in the preparation of FA- and FI-modified Au DENPs is to keep the surface charge on the particles neutral in order to avoid toxicity and nonspecific binding. This can be accomplished by a final acetylation step to convert the remaining amine groups of G5·NH_2 dendrimers to acetamides (Figure 1). Zeta-potential measurements show that after the final acetylation step, the surface potentials of the formed {$(Au^0)_{51.2}$-G5-FI_5-Ac} ($\xi = -1.11$ mV) and {$(Au^0)_{51.2}$-G5-FI_5-FA_5-Ac} ($\xi = -2.30$ mV) DENPs (Ac denotes acetyl) are close to neutral, indicating the success of the acetylation reaction. The slightly negative charges on both DENPs may derive from the deprotonated carboxyl groups in both FI and FA moieties being conjugated. The number of FI and FA moieties conjugated onto each Au DENP can be estimated by comparing the difference between the integration values of the ^{1}H NMR signals associated with the dendrimers and the FI and FA moieties, as we did for dendrimer (without entrapped Au nanoparticles) conjugation (Figure S1 in the Supporting Information).[13,19] The average number of FI and FA moieties conjugated onto each Au DENP was estimated to be 4.0 and 4.5, respectively.

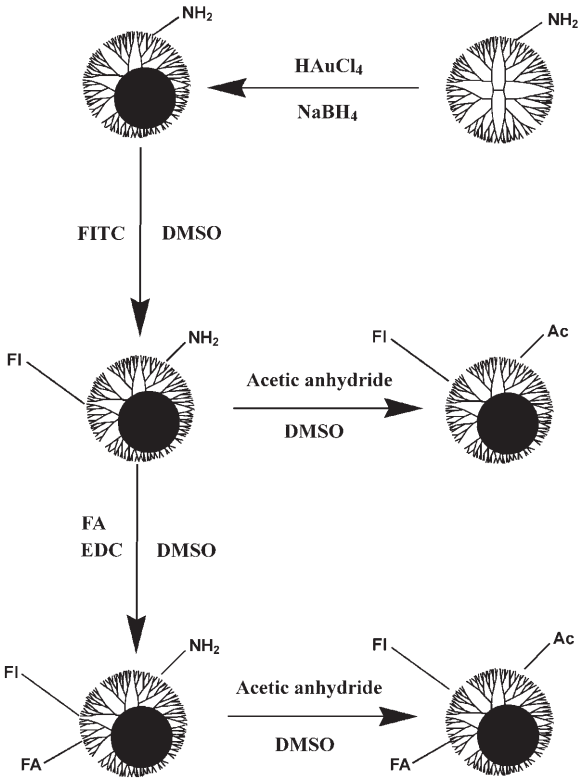

Figure 1. Schematic representation of the reactions involved in modifying Au DENPs for cancer-cell targeting and imaging.

Transmission electron microscopy (TEM) images show that the sizes of {$(Au^0)_{51.2}$-G5-FI_5-Ac} and {$(Au^0)_{51.2}$-G5-FI_5-FA_5-Ac} DENPs are 3.4 ± 0.6 nm and 3.2 ± 0.7 nm (Figure 2a–d), respectively. The larger sizes compared to those of pristine {$(Au^0)_{51.2}$-G5·NH_2} DENPs (2.1 nm)[11] may be because of multiple surface modifications, which facilitate Ostwald ripening of the Au DENPs. UV/Vis spectroscopy (Figure 2e) verified the conjugation of FI and FA moieties onto Au DENPs. The {$(Au^0)_{51.2}$-G5-FI_5-FA_5-Ac} DENPs show characteristic absorption peaks at both 500 nm and 280 nm for the FI and FA moieties, respectively, while only the characteristic absorption peak at 500 nm related to the FI moiety is observed for the {$(Au^0)_{51.2}$-G5-FI_5-Ac} DENPs. In addition, a band representing an overlap of the surface plasmon resonance of Au DENPs (510 nm) with the absorption of FI moieties is also observed. The functionalized Au DENPs are stable in both water solution and cell-culture medium, and no precipitation of the solution appeared even after periods of storage as long as 9 months (a photograph of the aqueous solutions of {$(Au^0)_{51.2}$-G5-FI_5-Ac} and {$(Au^0)_{51.2}$-G5-FI_5-FA_5-Ac} DENPs is shown in Figure S2 in the Supporting Information).

The stability of functionalized Au DENPs was also studied under different conditions. The UV/Vis spectra of {$(Au^0)_{51.2}$-G5-FI_5-Ac} and {$(Au^0)_{51.2}$-G5-FI_5-FA_5-Ac} DENPs dissolved in PBS buffer (Figure S3a, Supporting Information) do not show significant changes compared to those of the corresponding Au DENPs dissolved in water (Figure 2e), indicating that the ionic strength of the PBS buffer

NANO MICRO small

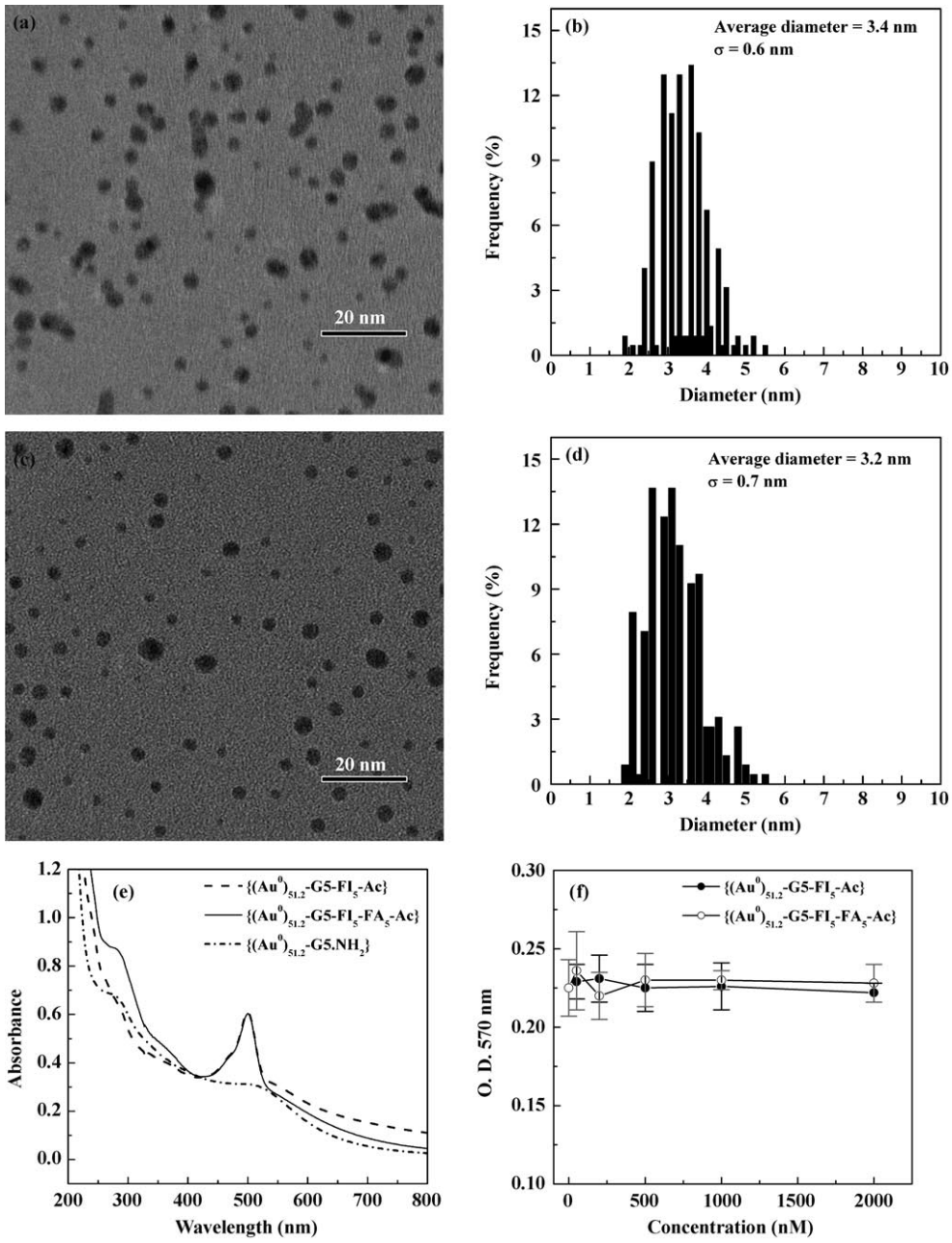

Figure 2. Characterization and toxicity test of functionalized Au DENPs. a, c) TEM images of the functionalized $\{(Au^0)_{51.2}$-G5-FI_5-Ac$\}$ and $\{(Au^0)_{51.2}$-G5-FI_5-FA_5-Ac$\}$ DENPs, respectively. b, d) Size-distribution histograms of $\{(Au^0)_{51.2}$-G5-FI_5-Ac$\}$ and $\{(Au^0)_{51.2}$-G5-FI_5-FA_5-Ac$\}$ DENPs, respectively. e) UV/Vis spectra of the starting $\{(Au^0)_{51.2}$-G5·$NH_2\}$ and functionalized $\{(Au^0)_{51.2}$-G5-FI_5-Ac$\}$ and $\{(Au^0)_{51.2}$-G5-FI_5-FA_5-Ac$\}$ DENPs. f) MTT assay of KB cell viability after treatment with $\{(Au^0)_{51.2}$-G5-FI_5-Ac$\}$ and $\{(Au^0)_{51.2}$-G5-FI_5-FA_5-Ac$\}$ DENPs for 24 h. The data are expressed as mean ± standard deviation.

does not have an impact on the stability of the Au DENPs. In addition, in solutions with pH values ranging from 5.3 to 8.4, both $\{(Au^0)_{51.2}$-G5-FI_5-Ac$\}$ and $\{(Au^0)_{51.2}$-G5-FI_5-FA_5-Ac$\}$ DENPs show similar absorbance profiles to those of the corresponding Au DENPs dissolved in water (Figure S3b and S3c), suggesting that the functionalized Au DENPs are stable and no aggregation is seen under the pH conditions studied. The morphologies of the functionalized Au DENPs at different pH conditions were also studied by TEM imaging (data not shown), further confirming that the Au DENPs are stable and have similar sizes and size distributions. This is consistent with our previous results for synthetically modified Au DENPs.[11] A 3-(4,5-dimethylthiazol-2-yl)-2,5-diphenyltetrazolium bromide (MTT) assay of KB cells shows that the functionalized Au DENPs are not cytotoxic even at concentrations up to 2000 nM (Figure 2 f), implying that the final acetylation step creates biocompatible nanoparticles.

2.2. Molecular-Dynamics Simulations of Surface-Modified Au DENPs

Molecular-dynamics simulations of pristine $\{(Au^0)_{51.2}$-G5·$NH_2\}$ DENPs and FA- and FI-modified $\{(Au^0)_{51.2}$-G5-FI_5-FA_5-Ac$\}$ DENPs were performed using conditions found to be optimal in previous studies to predict PAMAM dendrimers.[18,20] The dendrimer as a whole presents an extended structure because of the positively charged primary amines at pH 7, while easily containing the 2 nm Au sphere within (one of the equilibrated $\{(Au^0)_{51.2}$-G5·$NH_2\}$ DENP configurations is shown in Figure S4a of the Supporting Information). In order to incorporate the TEM data in the simulation (Figure 2), we used a 3-nm-diameter Au sphere for the $\{(Au^0)_{51.2}$-G5-FI_5-FA_5-Ac$\}$ DENP model. We randomly selected five primary amine groups for FI and another five for FA modification from the readily available primary amines of the Au DENP configuration. After attaching FI and FA molecules to the model, we modified the remaining primary amines into acetylated terminal groups. Figure S4b shows the potential energy changes over the simulation times for the $\{(Au^0)_{51.2}$-G5·$NH_2\}$ DENP and $\{(Au^0)_{51.2}$-G5-FI_5-FA_5-Ac$\}$ DENP models, respectively. Simulations were well equilibrated before the simulation time at 40 ps. One of the equilibrated configurations of $\{(Au^0)_{51.2}$-G5-FI_5-FA_5-Ac$\}$ DENP containing a 3 nm Au sphere is shown in Figure S4c (Supporting Information). The neutralized dendrimer shows a collapsed shape compared to the pristine $\{(Au^0)_{51.2}$-G5·$NH_2\}$ DENPs seen in Figure S4a, but the Au sphere is practically within the FA- and FI-modified G5 dendrimer, even with a larger Au particle (3 nm).

Interestingly, most FA moieties (pink spheres in Figure S4c) extend substantially outward, thus becoming available for interaction with the folic acid receptors (FAR) on the surface of the cells. Most FI moieties (green spheres in Figure S4c) are distant from the Au sphere, minimizing the fluorescence quenching effect with the Au. Figure S4d shows the density distribution of all atoms comprising FA (pink line) and FI (green line) from the center of mass of the $\{(Au^0)_{51.2}$-G5-FI_5-FA_5-Ac$\}$ DENP during 40 ps to 100 ps simulation times. The dotted line represents the mean radius of gyration (22.3 ± 0.04 Å) of the $\{(Au^0)_{51.2}$-G5-FI_5-FA_5-Ac$\}$ DENPs during the same simulation period. More than half of the FA moieties reside outside of the radius of gyration during these simulation times, confirming the availability of FA moieties for the binding with FAR on the surface of targeted cells.

2.3. Targeting of Functionalized Au DENPs to Cancer Cells Overexpressing Folate Receptors

FA has been extensively investigated for targeting various cancer cells, including ovary, kidney, uterus, testis, brain, colon, lung, and myelocytic blood that overexpress FAR.[21–24] The high-affinity FAR for FA ($K_d = 0.1$–1 nM) affords specific binding and internalization of FA-modified nanoparticles to cancer cells in the presence of normal cells through receptor-mediated endocytosis. KB cells were selected for the specific binding with functionalized Au DENPs. KB cells with both high and low levels of FAR were respectively incubated with $\{(Au^0)_{51.2}$-G5-FI_5-FA_5-Ac$\}$ and $\{(Au^0)_{51.2}$-G5-FI_5-Ac$\}$ DENPs for 1 h. Figure 3a–d shows the flow cytometric analyses of KB cells that express both high and low levels of FAR after exposure to functionalized Au DENPs (25 nM) for 1 h. It is clear that the treatment of KB cells expressing a high level of FAR with $\{(Au^0)_{51.2}$-G5-FI_5-FA_5-Ac$\}$ DENPs results in a significant increase in the fluorescence signal within the cells. In contrast, the same KB cells treated with $\{(Au^0)_{51.2}$-G5-FI_5-Ac$\}$ DENPs without FA display a similar fluorescence signal to cells treated with PBS buffer (Figure 3a), suggesting no binding of the $\{(Au^0)_{51.2}$-G5-FI_5-Ac$\}$ DENPs. KB cells with a low level of FAR treated with either $\{(Au^0)_{51.2}$-G5-FI_5-FA_5-Ac$\}$ or $\{(Au^0)_{51.2}$-G5-FI_5-Ac$\}$ DENPs show a similar fluorescence intensity to the PBS control (Figure 3b). These results indicate that the specificity of $\{(Au^0)_{51.2}$-G5-FI_5-FA_5-Ac$\}$ DENPs binding to KB cells is restricted to cells containing high levels of FAR. The cellular uptake of the FA-functionalized Au DENPs shows a dose-dependent trend, with saturation and 50% binding occurring at approximately 50 nM and 18 nM, respectively (Figure 3c), which is comparable with the binding capacity of FA-modified G5 dendrimers.[14] For KB cells with a low level of FAR, neither $\{(Au^0)_{51.2}$-G5-FI_5-FA_5-Ac$\}$ nor $\{(Au^0)_{51.2}$-G5-FI_5-Ac$\}$ DENPs show any significant binding, even at concentrations up to 300 nM (Figure 3d).

The conjugation of the FI moiety onto Au DENPs also enables confocal microscopic imaging of the intracellular uptake. Figure 3e–g shows that only KB cells with a high level of FAR treated with FA-modified $\{(Au^0)_{51.2}$-G5-FI_5-FA_5-Ac$\}$ DENPs display fluorescence signals, which is associated with the specific internalization of $\{(Au^0)_{51.2}$-G5-FI_5-FA_5-Ac$\}$ DENPs into the cytoplasm of the cells (Figure 3g). In contrast, the same KB cells treated with $\{(Au^0)_{51.2}$-G5-FI_5-Ac$\}$ DENPs without FA modification do not show any fluorescence signals (Figure 3f), which is the same as for KB cells treated with PBS buffer (Figure 3e). This result suggests that the binding and intracellular uptake do not occur in the cells treated with non-FA modified Au DENPs.

By using the TEM imaging technique, we can clarify the distribution of functionalized Au DENPs in different subcellular compartments inside targeted cells. Upon 2 h incubation of functionalized Au DENPs, the FA-modified $\{(Au^0)_{51.2}$-G5-FI_5-FA_5-Ac$\}$ DENPs were predominantly located in the lysosomes of KB cells with high-level FAR expression (Figure 4a and 4b). We also observed that a small portion of $\{(Au^0)_{51.2}$-G5-FI_5-FA_5-Ac$\}$ DENPs situated in vacuoles and the nucleus (Figures S5 and S6 of the Supporting Information). However, we did not see any uptake of the $\{(Au^0)_{51.2}$-G5-FI_5-Ac$\}$ DENPs without FA modification in the lysosomes of the same KB cells (Figure 4c). A very small quantity of $\{(Au^0)_{51.2}$-G5-FI_5-Ac$\}$ DENPs were observed in the vacuoles of some cells (Figure S7), but this was undetectable using confocal microscopy. This uptake is believed to be associated with diffusion-driven nonspecific binding since control cells not exposed to Au DENPs show no internalized metal nanoparticles (images not shown). The TEM studies highlighted the high specificity of FA-

NANO MICRO small

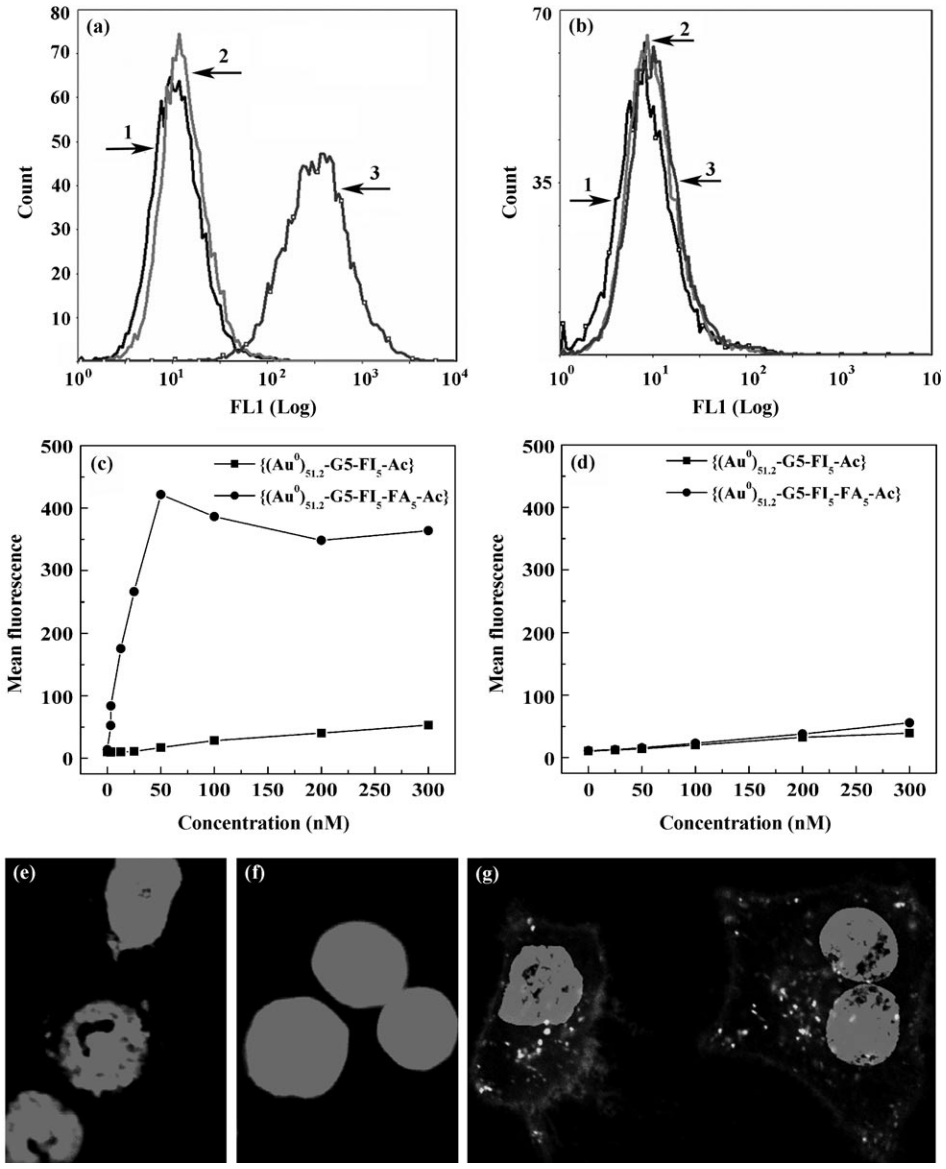

Figure 3. Flow cytometric and confocal microscopy studies of the binding of functionalized Au DENPs with KB cells. a, b) Binding of $\{(Au^0)_{51.2}$-G5-FI_5-Ac$\}$ and $\{(Au^0)_{51.2}$-G5-FI_5-FA_5-Ac$\}$ DENPs (25 nM) with KB cells with high and low levels of FAR, respectively: 1) PBS control; 2) $\{(Au^0)_{51.2}$-G5-FI_5-Ac$\}$; 3) $\{(Au^0)_{51.2}$-G5-FI_5-FA_5-Ac$\}$. c, d) Dose-dependent binding of $\{(Au^0)_{51.2}$-G5-FI_5-Ac$\}$ and $\{(Au^0)_{51.2}$-G5-FI_5-FA_5-Ac$\}$ DENPs with KB cells expressing high and low levels of FAR, respectively. e–g) Confocal microscopy images of KB cells with high-level FAR treated with PBS buffer (e), $\{(Au^0)_{51.2}$-G5-FI_5-Ac$\}$ (25 nM) (f), and $\{(Au^0)_{51.2}$-G5-FI_5-FA_5-Ac$\}$ (25 nM) (g) DENPs for 2 h, respectively.

modified Au DENPs for targeting KB cells with high-level FAR expression, and corroborate the confocal imaging data.

3. Discussion

The well-defined structure and composition, as well as the narrow polydispersity of dendrimers lead to their extensive applications for targeted cancer therapeutics.[12–14,25] However, dendrimer-based therapeutics do not allow the direct imaging of subcellular compartments because of the low electron-density contrast. One major advantage of using functionalized Au DENPs to image cancers is their ability to differentiate cancer cells from surrounding cells or tissues by using contrast agents with high electron density. The use of Au DENPs also aids in understanding the mechanism for targeted drug delivery and therapeutics, using dendrimer-based nanodevices. In addition, it is possible to use Au DENPs for laser hyperthermia cancer therapeutics through inductive heating of cancer cells that specifically internalize the particles.

Our previous work[11] shows that Au DENPs can be modified through reactions with dendrimer peripheral groups, while keeping a similar particle size and size distribution to the pristine amine-terminated Au DENPs. As compared to general short-range organic reactions, the modification of FI and FA molecules on the G5 dendrimer surface in the presence of Au nanoparticles may introduce strong hydrogen-bonding interactions between the linked moieties and water in solution. Therefore, the dendrimer skeletons that entrap Au nanoparticles may be more open and facilitate the Ostwald ripening process, thereby leading to an increase in size of the Au nanoparticles (3.2 nm for $\{(Au^0)_{51.2}$-G5-FI_5-FA_5-Ac$\}$ versus 2.1 nm for $\{(Au^0)_{51.2}$-G5·$NH_2\}$ DENPs, Figure 2). The increase of Au-nanoparticle size of the DENP structure does not have an impact on the stability of the particles in PBS buffer and in the pH ranges (5.3–8.4) studied (Figure S3). Our molecular-dynamics simulation studies show that the attached FI moieties on Au DENP surfaces are distant from the Au nanoparticles, which minimize the fluorescence quenching effect with metal Au, while the attached FA moieties extend substantially outward, thus becoming available for interaction with FAR on the surface of target cells (Figure S4). These properties allow the Au DENPs to perform perfectly in the binding and detection of cancer cells through receptor–ligand interactions (Figure 3 and Figure 4).

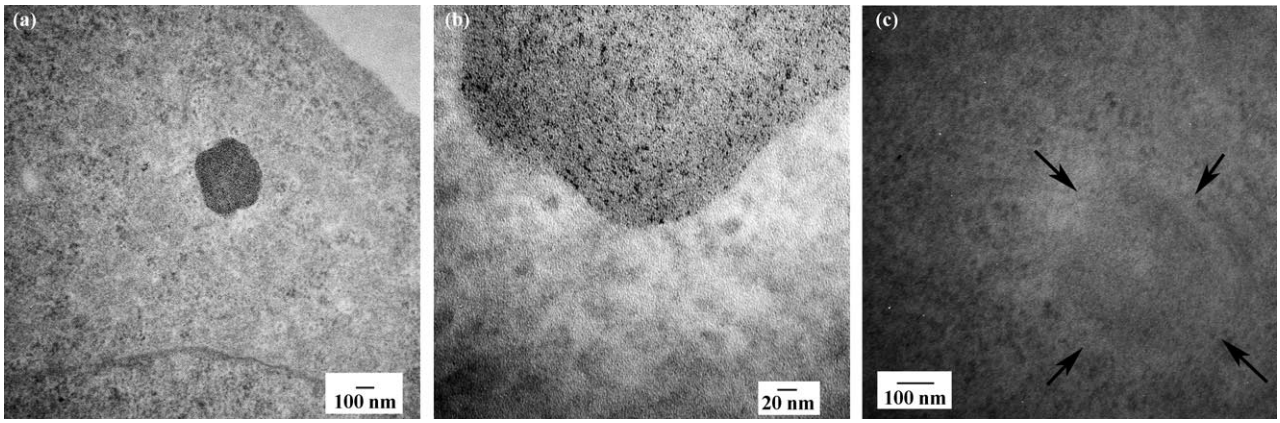

Figure 4. TEM images of cellular uptake of Au DENPs. a–c) TEM images of KB cells with high-level FAR treated with $\{(Au^0)_{51.2}$-G5-FI_5-FA_5-Ac$\}$ (a, b) and $\{(Au^0)_{51.2}$-G5-FI_5-Ac$\}$ DENPs (c) for 2 h, respectively. b) A magnified area of the lysosome of the same cell shown in (a). In (c), arrows indicate the lysosome morphology. The concentration for both Au DENPs is maintained at 50 nM.

4. Conclusions

In summary, we demonstrate that preformed Au DENPs prepared using amine-terminated G5·NH_2 dendrimers as templates can be covalently linked with FA and FI moieties through reaction with the terminal amines of G5·NH_2 dendrimer templates in the presence of entrapped Au nanoparticles. The functionalized Au DENPs are stable, biocompatible, and can be used for specific targeting and imaging of cancer cells with overexpressing FAR. We are currently doing extensive in vivo experiments to verify the in vivo performance of the functionalized Au DENPs. This approach to functionalizing Au DENPs may be applied to various other biological ligands (e.g., sugars, peptides, proteins, and antibodies) for targeting and imaging various biological systems. We also anticipate that drug molecules can be conjugated onto Au DENPs, thereby providing an approach for imaging and targeted treatment to various forms of cancers and biological systems.

5. Experimental Section

Synthesis and functionalization of Au DENPs: The procedure to synthesize Au DENPs is adopted from those previously reported in the literature, but with slight variations.[8,16] Details can be found in our previous report.[11] The Au DENPs were prepared using sodium borohydride reduction chemistry with the dendrimer terminal amine/gold atom molar ratio at 1:0.4. Briefly, a $HAuCl_4$ solution (118.2 mM, 5 mL) was added into a G5·NH_2 dendrimer (Dendritech, Midland, MI) aqueous solution (0.577 mM, 20 mL) under vigorous stirring. After 30 min, a $NaBH_4$ solution (197 mM, 6 mL) dissolved in a water/methanol (2:1 in volume) mixture was slowly added to the gold salt/dendrimer mixture while stirring. The reaction mixture turned a deep-red color within a few seconds after addition of the $NaBH_4$ solution. The stirring was continued for 2 h to complete the reaction. The reaction mixture was extensively dialyzed against water (six times, 4 L) for 3 days to remove the excess reactants, followed by lyophilization to obtain the product $\{(Au^0)_{51.2}$-G5·$NH_2\}$ DENPs.

Five molar equivalents of FI (3.27 mg, 8.4 μmol; Aldrich) dissolved in dimethylsulfoxide (DMSO; 5 mL) were added dropwise to a solution of $\{(Au^0)_{51.2}$-G5·$NH_2\}$ DENPs (61.19 mg, 1.68 μmol) in DMSO (10 mL) under a nitrogen atmosphere with vigorous magnetic stirring. After 24 h, the reaction mixture (15 mL) was divided into two aliquots with equal volume (7.5 mL). For aliquot 1, the FI-labeled $\{(Au^0)_{51.2}$-G5·$NH_2\}$ DENPs were acetylated to convert the remaining amino groups of the G5 dendrimer to acetamide groups according to a procedure in the literature.[26] Briefly, aliquot 1 was put together with triethylamine (37.4 mg, 0.37 mmol) and mixed well, followed by dropwise addition of an acetic anhydride solution (37.74 mg, 0.37 mmol) under vigorous stirring. After 24 h, the reaction mixture was extensively dialyzed against PBS buffer (three times, 4 L) and water (three times, 4 L) using a regenerated cellulose dialysis membrane (MWCO = 10 000; Fisher) for 3 days to remove the excess reactants and byproducts, followed by lyophilization to obtain the product $\{(Au^0)_{51.2}$-G5-FI_5-Ac$\}$ DENPs (yield = 59.3 %). ^{1}H NMR (500 MHz, D_2O) δ [ppm]: 6.99 (bs, 2 H), 6.39 (bs, 4 H), 3.10 (s, 174 H), 2.67 (s, 107 H), 2.43 (s, 73 H), 2.25 (s, 118 H), 1.78 (s, 102 H). The number of dendrimer protons was extrapolated based on the integration values relative to those for FI protons. The same situation applies for the FA modification with Au DENPs (see below).

For aliquot 2, the FI-labeled $\{(Au^0)_{51.2}$-G5·$NH_2\}$ DENPs were further modified with FA (Aldrich) according to a previous procedure with a slight modification.[15] Briefly, a 5-molar equivalent of FA (1.90 mg, 4.3 μmol; Aldrich) in DMSO (2 mL) was mixed with a DMSO solution (2 mL) containing *N*-(3-dimethylaminopropyl)-*N*′-ethylcarbodiimide hydrochloride (EDC) (34.8 μmol, 6.67 mg; Aldrich) and stirred for 3 h. This process activated the γ-carboxylic acid of FA for further reaction with FI-labeled $\{(Au^0)_{51.2}$-G5·$NH_2\}$ DENPs. The activated FA solution (4 mL in DMSO) was added to aliquot 2-FI-labeled $\{(Au^0)_{51.2}$-G5·$NH_2\}$ DENPs and stirred for 3 days. Then, the FI- and FA-modified

NANO MICRO small

$\{(Au^0)_{51.2}$-G5·$NH_2\}$ DENPs were further acetylated to neutralize the remaining amino groups of G5 dendrimers as described above, followed by extensive dialysis against PBS buffer (three times, 4 L) and water (three times, 4 L) for 3 days to remove the excess reactants and byproducts and lyophilization to obtain the product $\{(Au^0)_{51.2}$-G5-Fl_5-FA_5-Ac$\}$ DENPs (yield = 77.1 %). ^{1}H NMR (500 MHz, D_2O) δ [ppm]: 8.60 (bs, 1 H), 7.46 (bs, 2 H), 6.93 (bs, 2 H), 6.50 (bs, 2 H), 6.37 (bs, 4 H), 3.09 (s, 174 H), 2.66 (s, 107 H), 2.48 (s, 73 H), 2.23 (s, 118 H), 1.78 (s, 102 H).

Simulation conditions: All dendrimer models were built on an Onyx workstation (Silicon Graphics, Inc.; Mountain View, CA) using the Insight II software package (Accelrys, Inc.; San Diego, CA). All primary amines were protonated and carboxyl groups deprotonated to simulate pH 7 conditions. Since a Au crystal comprises a cubic close-packed structure, we prepared Au spheres with such a structure and applied constraints to fix their structures during the simulations. After the steepest descent minimization process for 5000 steps, MD simulations were performed at 1000 K for 5 ps followed by 100 ps runs (50 ps for the case of PAMAM dendrimer alone) with a 1 fs step at 300 K, using a consistent valence force field (CVFF) in the Insight II software. The potential energies stabilized much earlier than 50 ps. The total potential energy function (U_{total}) for MD calculations includes bonded terms (U_{bonded}: empirical potential energy terms describing chemical bonds) and nonbonded interactions ($U_{nonbonded}$), which is described as

$$U_{total} = U_{bonded} + U_{nonbonded} = U_{bonded} + U_{Lennard-Jones} + U_{Coulomb} = U_{bonded} + \frac{1}{2}\sum_i \sum_j \{\varepsilon[(\frac{\sigma}{r})^{12} - 2(\frac{\sigma}{r})^6] + \frac{q_i q_j}{Dr}\} \quad (1)$$

where ε is the minimum energy of the Lennard–Jones potential, σ the distance yielding a minimum Lennard–Jones potential, q the partial charge on the atom, D the dielectric constant (1 for vacuum), r the distance between i and j, and i, j are nonbonded atom pairs. We used the dielectric constant $D = r$, so that it can be a function of r. No long-range interaction cut-off was used, based on previous findings.[20]

Instrumentation for characterization of functionalized Au DENPs: ^{1}H NMR spectra of Au DENPs were recorded on a Bruker DRX 500 nuclear magnetic resonance spectrometer. Samples were dissolved in D_2O before NMR measurements. UV/Vis spectra were collected using a Perkin–Elmer Lambda 20 UV/Vis spectrometer. All samples were dissolved in water at a concentration of 1 mg mL^{-1}. Zeta-potential measurements were performed using a Malvern Zetasizer Nano ZS model ZEN3600 (Worcestershire, UK) equipped with a standard 633 nm laser. A JEOL 2010F analytical electron microscope was used at 200 kV with an EDS system attached. A 5 μL aqueous solution of Au DENPs (1 mg mL^{-1}) was dropped onto a carbon-coated copper grid and air dried before measurements.

Cell cultures and biological evaluation: The KB cells (ATCC, CLL17, Rockville, MD) were continuously grown in two 24-well plates, one in FA-free media and the other in regular RPMI 1640 cell culture medium (Gibco/BRL, Gaithersburg, MD) supplemented with penicillin (100 units mL^{-1}; Sigma, St. Louis, MO), streptomycin (100 μg mL^{-1}; Sigma), 10 % heat-inactivated FBS, and 2.5 μM FA. The cells grown in FA-free media express high-level FAR, while the cells grown in FA-containing media express low-level FAR.

MTT cytotoxicity assay: An MTT (3-(4,5-dimethylthiazol-2-yl)-2,5-diphenyltetrazolium bromide) assay was used to quantify the viability of cells. Briefly, $\approx 5 \times 10^4$ KB cells per well were seeded into a 96-well plate. After overnight incubation, functionalized Au DENPs at concentrations ranging from 0 to 2 μM in PBS (pH 7.4) were added. After 24 h incubation with Au DENPs at 37 °C, the MTT reagent in PBS solution was added. The assays were carried out according to the manufacturer's instructions. For each concentration of Au DENPs, five wells of cells were analyzed.

Flow cytometry analysis: Approximately 2×10^6 cells per well were seeded in 12-well plates the day before the experiments. An hour before initiating an experiment, the cells were rinsed four times with serum-free and FA-deficient RPMI 1640 media. Functionalized Au DENPs were added in the final concentrations of 0–300 nM. After 1 h incubation with the functionalized Au DENPs, KB cells with both high- and low-level FAR expression were trypsinized (Gibco/BRL, Gaithersburg, MD) and suspended in PBS containing 0.1 % bovine serum albumin (Sigma, St. Louis, MO) and analyzed using a Becton Dickinson FACScan analyzer. The FL1-fluorescence of 10 000 cells was measured, and the mean fluorescence of gated viable cells was quantified.

Confocal microscopy: Confocal microscopic analysis was performed in cells plated on a plastic cover-slip using an Olympus FluoView 500 laser scanning confocal microscope (Melville, NY). Fl fluorescence was excited with a 488 nm argon blue laser and emission was measured through a 505–525 barrier filter. The optical section thickness was set at 5 μm. The cells were incubated with functionalized Au DENPs for 2 h, followed by rinsing with PBS buffer. The nuclei were counterstained with 1 μg mL^{-1} of Hoescht 33342, using a standard procedure. Samples were scanned using a 60× water-immersion objective lens and magnified with FluoView software.

Transmission electron microscopy (TEM): The uptake of functionalized Au DENPs was further examined by a Phillips CM 100 electron microscope operating at a voltage of 60 kV. Images were recorded using a Hamamatsu digital camera controlled by AMT (advance microscopy technology) software. The specimens were prepared according to the following procedures. The KB cells with high-level FAR were aliquoted in 5 mL tubes at a concentration of 1×10^6 cells mL^{-1}. After overnight growth at 37 °C, the medium was removed and 2 % FBS solution containing 50 nM of functionalized Au DENPs was added; the incubation was carried out for 2 h at 37 °C. Then, the medium was removed and cells were washed with Sorenson buffer and fixed at room temperature for 1 h using 2.5 % of glutaraldehyde in Sorenson buffer. The cells were rinsed 3 times with Sorenson buffer, resuspended in the same medium, and post-fixed using 1.0 % osmium tetroxide for 1 h. After additional washing in buffer, the cells were dehydrated in a series of ethanol solutions of 30 %, 50 %, 70 %, 95 %, and 100 %. The samples were further infiltrated using the following sequence of mixtures of 100 % ethanol and Epon: 3 parts of ethanol + 1 part resin (for 1 h), 1 part of ethanol + 1 part resin (for 1 h), 1 part of ethanol + 3 parts resin (overnight), full-strength resin (4 h), and full-strength resin (overnight). After the third change of resin, polymerization was performed and sections with the thickness of 75 nm were ob-

tained using a Reichart Ultramicrotome. Sections were mounted on 200-mesh copper grids before TEM measurements.

Acknowledgements

This work is financially supported by the National Cancer Institute (NCI), National Institute of Health (NIH), under the contract number NOI-CO-97111. The 2010F microscope used in the study was funded by NSF through the Grant DMR-9871177. We thank Prof. Younan Xia and Alejandro L. Briseno at the University of Washington for helpful discussions.

[1] L. Balogh, D. A. Tomalia, *J. Am. Chem. Soc.* **1998**, *120*, 7355 – 7356.
[2] R. M. Crooks, M. Zhao, L. Sun, V. Chechik, L. K. Yeung, *Acc. Chem. Res.* **2001**, *34*, 181 – 190.
[3] M. Zhao, L. Sun, R. M. Crooks, *J. Am. Chem. Soc.* **1998**, *120*, 4877 – 4878.
[4] F. Grohn, B. J. Bauer, Y. A. Akpalu, C. L. Jackson, E. J. Amis, *Macromolecules* **2000**, *33*, 6042 – 6050.
[5] J. Zheng, J. T. Petty, R. M. Dickson, *J. Am. Chem. Soc.* **2003**, *125*, 7780 – 7781.
[6] R. W. J. Scott, O. M. Wilson, R. M. Crooks, *J. Phys. Chem. B* **2005**, *109*, 692 – 704.
[7] J. Zheng, C. Zhang, R. M. Dickson, *Phys. Rev. Lett.* **2004**, *93*, 077 402/1 – 077 402/4.
[8] A. Manna, T. Imae, K. Aoi, M. Okada, T. Yogo, *Chem. Mater.* **2001**, *13*, 1674 – 1681.
[9] A. Bielinska, J. D. Eichman, I. Lee, J. R. Baker, Jr., L. Balogh, *J. Nanopart. Res.* **2002**, *4*, 395 – 403.
[10] W. Lesniak, A. U. Bielinska, K. Sun, K. W. Janczak, X. Shi, J. R. Baker, Jr., L. P. Balogh, *Nano Lett.* **2005**, *5*, 2123 – 2130.
[11] X. Shi, S. Wang, H. Sun, J. R. Baker, Jr., *Soft Matter* **2007**, *3*, 71 – 74.
[12] J. F. Kukowska-Latallo, K. A. Candido, Z. Cao, S. S. Nigavekar, I. J. Majoros, T. P. Thomas, L. P. Balogh, M. K. Khan, J. R. Baker, Jr., *Cancer Res.* **2005**, *65*, 5317 – 5324.
[13] I. J. Majoros, T. P. Thomas, C. B. Mehta, J. R. Baker, Jr., *J. Med. Chem.* **2005**, *48*, 5892 – 5899.
[14] T. P. Thomas, I. J. Majoros, A. Kotlyar, J. F. Kukowska-Latallo, A. Bielinska, A. Myc, J. R. Baker, Jr., *J. Med. Chem.* **2005**, *48*, 3729 – 3735.
[15] Y. Choi, T. Thomas, A. Kotlyar, M. T. Islam, J. R. Baker, Jr., *Chem. Biol.* **2005**, *12*, 35 – 43.
[16] Y.-G. Kim, S.-K. Oh, R. M. Crooks, *Chem. Mater.* **2004**, *16*, 167 – 172.
[17] J. R. Baker, Jr., A. Quintana, L. T. Piehler, M. Banazak-Holl, D. Tomalia, E. Raczka, *Biomed. Microdevices* **2001**, *3*, 61 – 69.
[18] A. Quintana, E. Raczka, L. Piehler, I. Lee, A. Myc, I. Majoros, A. K. Patri, T. Thomas, J. Mule, J. R. Baker, Jr., *Pharm. Res.* **2002**, *19*, 1310 – 1316.
[19] X. Shi, I. Majoros, A. K. Patri, X. Bi, M. T. Islam, A. Desai, T. R. Ganser, J. R. Baker, Jr., *Analyst* **2006**, *131*, 374 – 381.
[20] I. Lee, B. D. Athey, A. W. Wetzel, W. Meixner, J. R. Baker, *Macromolecules* **2002**, *35*, 4510 – 4520.
[21] I. G. Campbell, T. A. Jones, W. D. Foulkes, J. Trowsdale, *Cancer Res.* **1991**, *51*, 5329 – 5338.
[22] P. Garin-Chesa, I. Campbell, P. E. Saigo, J. L. Lewis, Jr., L. J. Old, W. J. Rettig, *Am. J. Pathol.* **1993**, *142*, 557 – 567.
[23] D. Weitman, R. H. Lark, L. R. Coney, D. W. Fort, V. Frasca, V. R. Surawski, B. A. Kamen, *Cancer Res.* **1992**, *52*, 3396 – 3401.
[24] F. Ross, P. K. Chaudhauri, M. Ratnam, *Cancer* **1994**, *73*, 2432 – 2443
[25] I. J. Majoros, A. Myc, T. Thomas, C. B. Mehta, J. R. Baker, *Biomacromolecules* **2006**, *7*, 572 – 579.
[26] I. J. Majoros, B. Keszler, S. Woehler, T. Bull, J. R. Baker, Jr., *Macromolecules* **2003**, *36*, 5526 – 5529.

Received: January 22, 2007
Published online on May 24, 2007

